EPJ Web of Conferences **119**, 12003 (2016) DOI: 10.1051/epjconf/201611912003
ILRC 27

WINTER TEMPERATURE AND TIDAL STRUCTURES FROM 2011 TO 2014 AT MCMURDO STATION: OBSERVATIONS FROM FE BOLTZMANN TEMPERATURE AND RAYLEIGH LIDAR

Weichun Fong[1,2], Xinzhao Chu[1,2], Xian Lu[1], Timothy J. Fuller-Rowell[1,3], Mihail Codrescu[3], Arthur D. Richmond[4], Zhibin Yu[1,2], Brendan Roberts[1,2], and Cao Chen[1,2]

[1] *University of Colorado at Boulder, 216 UCB, CIRES, Boulder, CO 80309, USA.*
Email: weichun.fong@colorado.edu and Xinzhao.Chu@colorado.edu
[2]*Aerospace Engineering Sciences, University of Colorado, Boulder, CO, USA.*
[3] *SWPC, NOAA, Boulder, CO, USA.* [4] *HAO, NCAR, Boulder, CO, USA*

ABSTRACT

McMurdo station (77.8°S, 166.7°E), locating at the poleward edge of the auroral oval, provides great opportunities for researchers to study the interactions among neutral atmosphere, ionosphere and magnetosphere. More than four years of valuable data have been collected, leading to several new discoveries from the McMurdo lidar campaign. Presented here are the winter temperature tides and their responses to the magnetospheric sources. Winter temperature structures from the lidar observations are also presented for this high southern latitude.

1. INTRODUCTION

Polar middle and upper atmosphere is complex and is one of the least understood regions on the Earth. Between 100 and 200 km, the ion-neutral collisions have apparent altitude dependence due to the exponentially decay of the neutral density, therefore, the neutral constituents and their dynamics have large impacts on the plasma dynamics [1]. Meanwhile, the open geomagnetic field lines allow the energetic particles penetrate into the lower thermosphere or even mesosphere under strong geomagnetic disturbance, and the energy carried by these energetic particles eventually transfer into the ionosphere-thermosphere (IT) system. Such strong coupling between the polar IT system and the magnetosphere complicates the situation when considering the energy budget and dynamics, and it is still unclear that how magnetosphere energy is dissipated and distributed spatially and temporally in this region.

Atmospheric temperature, as one of the important parameters, dominates numerous geophysical phenomena and is also a key variable to climate change studies. Temperature and its variations in the polar IT region are not only affected by the energy propagating from the lower atmosphere but also strongly related to the magnetospheric energy dissipation. However, temperature measurements of the high latitude regions are rare comparing with those of middle and low latitudes. Very few ground-based instruments, especially active remote sensing ones, have made measurements at such high southern latitude so far due to the difficulty to access the harsh environment, and the spaceborne satellites are usually limited by their viewing geometry and cannot provide high resolution measurements.

McMurdo station (77.8°S, 166.7°E), sitting at the poleward edge of the auroral oval (Figure 1), provides a great opportunity for atmospheric scientists to study how neutral atmosphere interacts with the ionosphere and is affected by the magnetosphere. University of Colorado (CU) Lidar group has deployed an Fe Boltzmann lidar system at McMurdo since December 2010. The McMurdo lidar campaign is aiming to address these questions with high-quality observations for new science discoveries. The lidar system can be operated during both day and night, leading to full diurnal coverage. The lidar was operated at almost every clear sky since the day of installation, and over 4000 hours of data has been collected so far.

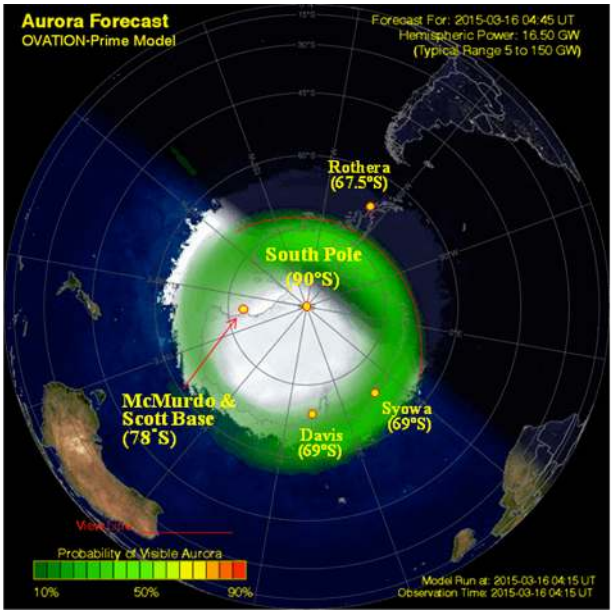

Figure 1. Map of Antarctica with aurora forecast, taken and modified from: http://www.swpc.noaa.gov/products/30-minute-aurora-forecast

In this paper, we introduce the lidar observational campaign in winter, and present the results of winter temperature and tidal structures at McMurdo.

2. LIDAR CAMPAIGN AT MCMURDO

2.1 Fe Boltzmann Lidar System

The lidar system was originally developed by Chu, Gardner and co-workers in 1998 at University of Illinois. It was deployed to the North Pole and the Arctic on board NSF/NCAR Electra aircraft in 1999, to the South Pole (1999–2001), and to Rothera (2002–2005). From 2009 to

2010, the lidar system was refurbished and upgraded by the University of Colorado lidar group. It was tested and collected data simultaneously with a Na Doppler lidar system co-located at Table Mountain Lidar Observatory, Boulder, Colorado in the summer of 2010. After that, the whole Fe system was shipped to McMurdo station, and has the lidar campaign started since December 16, 2010. One of the main purposes of the McMurdo lidar campaign is to fill in the data gap in between the South Pole (90°S) and Rothera (67.5°S) stations.

The lidar system consists of two independent channels of 372 and 374 nm, corresponding to the two absorption lines of atomic Fe. At the same time, each channel works individually as a Rayleigh lidar. The details of the refurbishment and upgrade of the lidar system could be found in [2]. Temperatures in the MLT region (80–110 km) can be derived from both channels using the Fe Boltzmann techniques based on the Maxwell-Boltzmann distribution law as shown in equation (1) [3], and from 30–70 km using the Rayleigh integration technique [4].

$$\frac{P_{374}}{P_{372}} = \frac{g_2}{g_1}\exp\left(-\Delta E \big/ k_B T\right) \quad (1)$$

P is the population of the state, g is the degeneracy factor, ΔE is the energy difference between the two states, k_B is the Boltzmann constant, and T is the temperature.

2.2 Winter Operation of Fe Lidar system

This Fe lidar system is a sophisticated system. For each winter, one member of CU lidar team will be deployed to McMurdo and stay 8 months through whole Antarctic winter. Most of the major maintenances and system tests are usually done in the summer, while the largest human power and access of the resources guarantee that the lidar system is kept at the best status for the coming winter. While entering the winter season, the operation of the system switches to the "campaign mode", which means only the essential maintenances will be performed on the system. The goal of the winter is to collect data as much as possible, weather permitting. Table 1 shows the statistics of the lidar data collected from April to September from the past four years. In average, over 60 hours/month of data were collected in 2011 and 2012, and over 80 hours/month in 2013 and 2014.

Table 1. Winter lidar observation statistics (2011–2014)

Month	April	May	June	July	Aug	Sept
2011	55(5)	59(6)	70(4)	48(3)	72(5)	31(4)
2012	70(7)	57(5)	85(5)	32(4)	32(3)	87(6)
2013	118(8)	57(5)	85(6)	90(5)	72(5)	76(5)
2014	54(5)	127(4)	147(5)	77(3)	25(4)	60(5)
Total	297(25)	300(20)	387(20)	247(15)	201(17)	254(20)

*The numbers indicate the total hours (episodes) of data collected in the corresponding month.

During winter, for most of the time, the system is operated in darkness (May to August) or has day and night alternation (April and September). In the total dark night, the solar background level is very low, and the photomultiplier tubes (PMT) receive near zero photon counts at background altitudes. Under such circumstance, three changes are made in the receiver chain for better and more stable signal levels: 1) the daytime etalon filter in between chopper and PMT is removed, 2) the interference filter is changed from 0.3 nm (pass-band width) to 4.2 nm, and 3) the 2-mm pinhole in front of the chopper is replaced with a 4-mm one to increase the equivalent field of view of the telescope. With the etalon removed and wider bandwidth of interference filter is used, the receiver optical efficiency increases by more than 3 times [5] and the larger pinhole decreases the fluctuation due to the transmitted beam swinging during lidar run.

Figure 2 shows an example of a 65-hour continuous lidar run by Cao Chen from June 28–30, 2014. In Figure 2, strong temperature perturbations between 85 and ~110 spanned the whole observation period. The peak-to-peak amplitude of perturbation is about 40 K at 90 km, and the oscillating periods are between 7 and 9 hours. Such strong temperature perturbations with periods between 4 and 10 hours were frequent observed during winter at McMurdo. The sources of these strong waves are still remaining unclear, but a strong candidate could be the inertia gravity wave (IGW) generated at stratosphere jet near 40 km. *Chen et al.* [6] reports the first coincident observation of IGWs by this Fe lidar and the co-located Scott Base medium frequency (MF) radar. Contrary to the high frequency oscillation structure in the MLT region, the Rayleigh temperature appears to have longer oscillating period, for which the period is greater than 2 days.

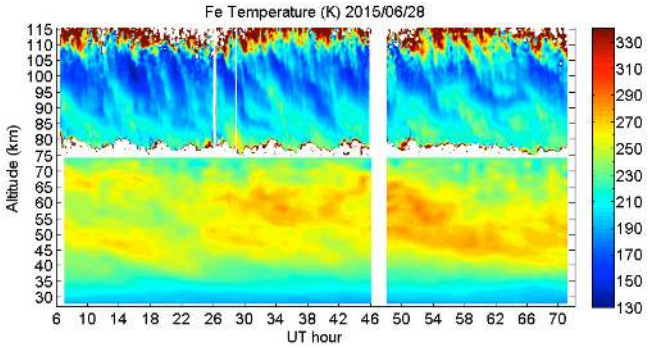

Figure 2. Temperature contour from 30 to 115 km at McMurdo from June 28–30, 2014. The lidar was run continuously for 65 hours.

From Figure 2, the altitude span of the temperature contour in the MLT region also indicates the distribution of the Fe layer in the MLT region. In order to derive robust temperature, the Fe density has to reach certain level. In the wintertime, the Fe layer usually spans from as low as 75 km to over 110 km. In some occasions, the Fe layer can extend as high as over 155 km [7].

3. WINTER TEMPERATURES AND TIDES

3.1 Winter Temperature Structures

Four years of temperature measurements enable us to investigate the winter temperature structure from 30 to 110 km. Figure 3 shows the lidar measurement of monthly mean temperatures from May to August in 2011-14. For each month, the temperature data were first binned to resolution of 1 km in altitude and 1 hour in time. Then the monthly average profile was calculated by taking the mean of the diurnal composite contour, which was formed by averaging the measurements with the same UT hour in the same month. Finally, the four-year monthly mean temperature (bold black in Figure 3) was obtained by simply averaging the four profiles from each year.

It can be seen that the four years lidar observations show similar winter mesopause and stratopause heights. The mean mesopause is at about 96–100 km and the stratopause is at about 51–53 km from May through August. The mean mesopause temperatures are between 180 and 190 K and the stratopause temperatures are between 260 and 275 K through four months. Comparing the monthly mean profiles of four years, it is clear that large inter-annual variations of temperature exist. Especially in the MLT region, for example, the mesopause temperature can have 20 K interannual variability in July.

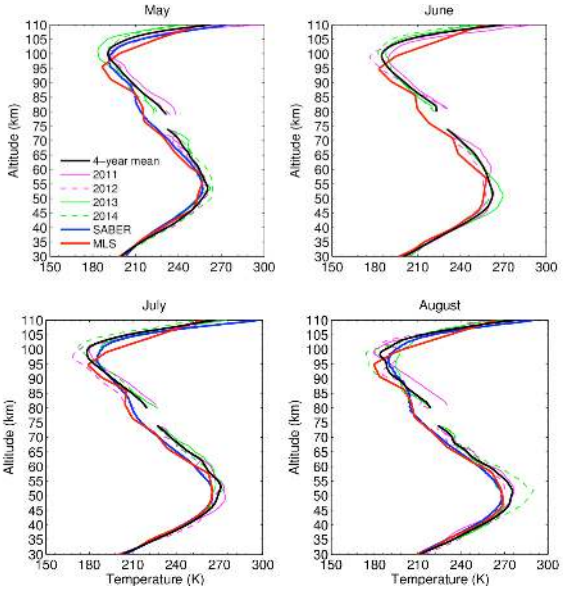

Figure 3. Monthly mean temperature profiles from 30 to 110 km at McMurdo from 2011 to 2014. The same periods of satellite measurements by SABER and MLS are plotted for comparison (no SABER data in June).

The lidar results are also compared to two satellite measurements, the Sounding of the Atmosphere using Broadband Emission Radiometry (SABER) experiment on TIMED satellite and the Microwave Limb Sounder (MLS) on the EOS Aura satellite. Both satellite measurements in each month are the mean of temperature profiles retrieved from 2011 to 2014 near McMurdo station. For most of the months, SABER has colder stratopause and warmer mesopause, but the heights of stratopause and mesopause are similar to the lidar measurements. Furthermore, above 100 km, SABER agrees with lidar measurement quite well. It is worth mentioning that SABER does not have measurements in June because of the yaw maneuver of the TIMED and the viewing geometry of SABER. MLS also exhibits colder stratopause than lidar. However, the vertical resolution of MLS in the MLT region is reduced to about 4 km, which could not provide trustable mesopause height and temperature. But generally speaking, the MLS appears to have similar mesopause temperatures as lidar.

3.2 Winter Temperature Tides

The winter temperature tides from the four years of lidar measurements are also investigated. Figure 4a shows the composite contour of temperature perturbations from 16 months lidar data of May through August through 2011 to 2014. Clear diurnal and semidiurnal features can be seen in the Rayleigh (30–70 km) and MLT (80–110 km) region, respectively. A harmonic fitting model comprising a mean temperature plus diurnal and semidiurnal tides was used to quantify the tidal structure. From Figure 5a, it can be seen that the diurnal tidal amplitudes are about 1–3 K below 100 km, but swiftly increase above 100 km. Semidiurnal tide also has small amplitudes (< 3 K) below 100 km (Figure not shown). The reconstructed composite contour from the diurnal and semidiurnal tides, as shown in Figure 4b, captures the major features of Figure 4a, indicating that the tidal information in Figure 5a and 5b are reasonable. The detailed data process procedures and discussions can be found in [8].

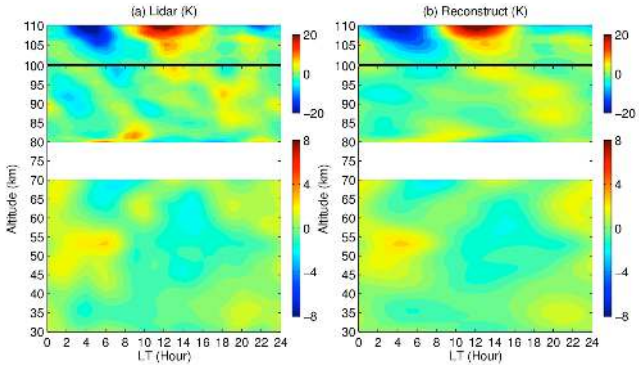

Figure 4. (a) Composite and (b) reconstructed contours of temperature perturbations from 2013 to 2014 data. The temperatures below and above 100 km are indicated by the bottom and top color bars, respectively.

The further investigation of the fast increase with altitude of the diurnal tidal amplitudes above 100 km reveals that the tidal sources are from magnetosphere instead of the source from lower atmosphere [9]. By separating the temperature data under different Kp index conditions, we found that the tidal amplitude increases in strength with the Kp magnetic activity index, as shown in Figure 5c and 5d. A global circulation model, the Coupled Thermosphere

Ionosphere Plasmasphere Electrodynamics (CTIPe) model, was used for the mechanistic studies of this tidal behavior.

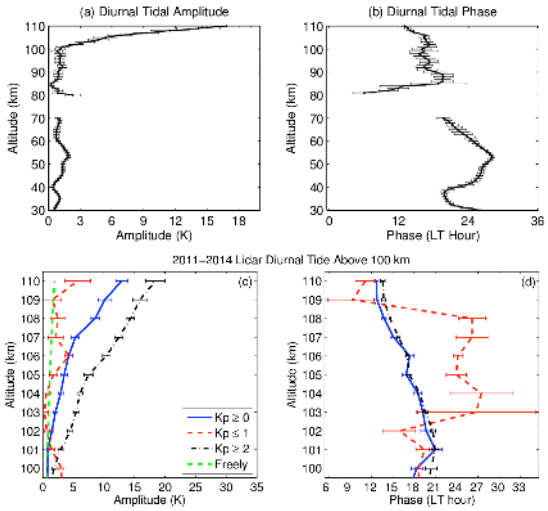

Figure 5. (a-b) Lidar observations of winter temperature diurnal tidal structures from 30 to 110 km and (c-d) tidal amplitudes and phases above 100 km under different Kp conditions at McMurdo from 2011 to 2014.

An interesting finding is that, between 100 and ~116 km, the model results show that the adiabatic cooling/heating associated with Hall ion drag is the dominant source of this feature. As shown in Figure 6, with the real-time run of the CTIPe model, the tidal amplitudes form a concentric ring structure circling the geomagnetic pole and overlap the auroral zone, which point to the magnetospheric source origin. The simulated tidal amplitudes are also comparable with those of the lidar observations. A test run was then launched with the Hall ion drag removed from the model. The results plotted in Figure 6 show that the tidal amplitudes significantly decrease, indicating that the Hall ion drag plays an important role in the lower thermosphere. The detailed discussion can be found in [9].

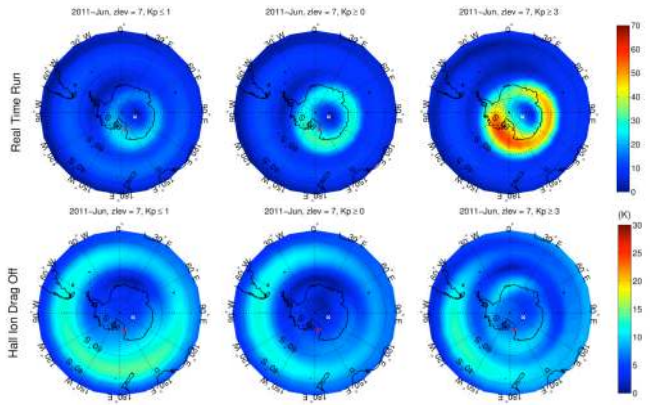

Figure 6. CTIPe model output of diurnal temperature tidal amplitudes at level 7 (~116 km). Upper row is the real-time run and lower row is without Hall ion drag in the model.

4. CONCLUSIONS

The McMurdo lidar campaign has provided invaluable data of the polar middle and upper atmosphere. The temperature measurements during winter not only fill in the data gap in between the South Pole and Rothera stations, but also can provide crucial information to the climate models and space weather forecast models. The measurements and studies of temperature tides above 100 km also help advance our understandings of the relation between IT system and the magnetosphere.

ACKNOWLEDGEMENTS

We acknowledge Wentao Huang, Zhangjun Wang, Chester Gardner, John Smith, Jian Zhao, and Ian Barry for their contributions to the project. We also thank the staff of United States Antarctica Program, McMurdo Station, Antarctica New Zealand, and Scott Base for their support. This project was supported by the USA National Science Foundation OPP grants ANT-0839091 and PLR-1246405. W. F. was partially supported by NSF grant AGS-1136272.

REFERENCES

[1] Richmond, A. D., and J. P. Thayer, 2000: Ionospheric electrodynamics: A tutorial, in *Magnetospheric Current Systems, Geophys. Monogr. Ser.*, *118*, pp. 131–146, edited by S.-I. Ohtani et al., AGU, Washington, D.C.

[2] Wang, Z. et al., 2012: Refurbishment and upgrade of Fe Boltzmann/Rayleigh temperature lidar at Boulder for a McMurdo lidar campaign in Antarctica, *Proc. of the 26th ILRC*, pp. 207–210, Porto Heli, Greece, June 2012.

[3] Gelbwachs, J. A., 1994: Iron Boltzmann factor LIDAR: proposed new remote-sensing technique for mesospheric temperature, *Applied Optics*, 33, 7151–7156.

[4] Hauchecorne, A. and M. Chanin, 1980: Density and temperature profiles obtained by lidar between 35 and 70 km, *Geophys. Res. Lett.*, 7(8), 565–568.

[5] Chu, X. et al., 2002: Fe Boltzmann temperature lidar: design, error analysis, and initial results at the North and South Poles. *Applied Optics 41* (21), 4400–4410.

[6] Chen, C. et al., 2013: Inertia-gravity waves in Antarctica: A case study using simultaneous lidar and radar measurements at McMurdo/Scott Base (77.8°S, 166.7°E), J. Geophys. Res. Atmos., 118, 2794–2808.

[7] Chu, X. et al., 2011: Lidar observations of neutral Fe layers and fast gravity waves in the thermosphere (110–155 km) at McMurdo (77.8°S, 166.7°E), Antarctica, *Geophys. Res. Lett.*, *38*, L23807.

[8] Fong, W. et al., 2014: Winter temperature tides from 30 to 110 km at McMurdo (77.8°S, 166.7°E), Antarctica: Lidar observations and comparisons with WAM, *J. Geophys. Res. Atmos.*, *119*.

[9] Fong, W. et al., 2015: Lidar and CTIPe model studies of the fast amplitude growth with altitude of the diurnal temperature "tides" in the Antarctic winter lower thermosphere and dependence on geomagnetic activity, *Geophys. Res. Lett.*, *42*, doi:10.1002/2014GL062784.